

# SCIENTIFIC REPORTS



OPEN

## States and traits of neural irregularity in the age-varying human brain

Leonhard Waschke , Malte Wöstmann  & Jonas Obleser 

Sensory representations, and thus human percepts, of the physical world are susceptible to fluctuations in brain state or “neural irregularity”. Furthermore, aging brains display altered levels of neural irregularity. We here show that a single, within-trial, information-theoretic measure (weighted permutation entropy) captures neural irregularity in the human electroencephalogram as a proxy for both, trait-like differences between individuals of varying age, and state-like fluctuations that bias perceptual decisions. First, the overall level of neural irregularity increased with participants’ age, paralleled by a decrease in variability over time, likely indexing age-related changes at structural and functional levels of brain activity. Second, states of higher neural irregularity were associated with optimized sensory encoding and a subsequently increased probability of choosing the first of two physically identical stimuli to be higher in pitch. In sum, neural irregularity not only characterizes behaviourally relevant brain states, but also can identify trait-like changes that come with age.

Brain activity, no matter if ongoing or evoked by sensory stimulation, is inherently variable or irregular — a phenomenon often termed “neural noise”<sup>1,2</sup>. The degree of this neural irregularity in neocortex is thought to track perceptual sensitivity<sup>3</sup>, but might also capture more lasting changes in brain activity that come with age. Moreover, neural irregularity is discussed as a potential marker of different neuropsychiatric disorders<sup>4</sup>. What has been missing so far, however, is a feasible and versatile metric of neural irregularity in the human EEG that would capture both, the trait-like, across-participants variations in neural irregularity and state-like, across-trials variations within the individual that co-determine the perceptual decisions we take facing ambiguous or missing physical evidence.

Across individuals, older age is accompanied by decreasing trial-to-trial brain signal variability<sup>5,6</sup> and increasing  $1/f$  noise in the electroencephalogram (EEG; i.e., flatter EEG frequency spectra)<sup>7,8</sup>. Those changes likely reflect a shift from distributed to more local processing<sup>9</sup>. Spontaneous brain activity, and in particular its variability, thus tracks stable, trait-like differences *between* individuals of varying age.

*Within* an individual, the (ir-)regularity of ongoing cortical activity might be a constituent of brain states that influence sensory encoding, perception, and ensuing behaviour. For instance, the neural response to a sensory stimulus depends on a participant’s cortical activity preceding stimulus onset<sup>2</sup>. More precisely, encoding and representing sensory information is more thorough in the presence of a desynchronized (irregular) state as compared to a synchronized (regular) state<sup>10,11</sup>. Intra-individual variability of spontaneous cortical activity hence represents fluctuations of cortical states that entail perceptual and behavioural relevance.

A desirable measure of neural irregularity should not only predict differences in encoding and perceptual decisions between identical stimuli (in terms of a neural state), but also track changes in the degree of irregularity that come with older age (in terms of a neural trait)<sup>3</sup>. The most promising measures in this respect, offering sufficient resolution in time and space, derive from information theory: Entropy measures have been used extensively to research epileptic seizures<sup>12,13</sup> or vigilance states<sup>14</sup> and cognitive processes in the EEG<sup>15</sup>. They offer an intuitive way of quantifying neural irregularity since with increasing versus decreasing irregularity of the EEG signal, entropy of the EEG will increase versus decrease, respectively. Information-theoretic measures of single trial time-courses should allow tracking whether neural irregularity (i) can be linked to perceptual decisions, reflecting trial-by-trial brain-state changes and (ii) can serve as a trait-like marker for individual age-related change

Department of Psychology, University of Lübeck, 23562, Lübeck, Germany. Correspondence and requests for materials should be addressed to L.W. (email: [leonhard.waschke@uni-luebeck.de](mailto:leonhard.waschke@uni-luebeck.de)) or J.O. (email: [jonas.obleser@uni-luebeck.de](mailto:jonas.obleser@uni-luebeck.de))

in brain activity. Here, we demonstrate that these requirements are met by a single-trial, time-resolved, ordinal measure of entropy, called Weighted Permutation Entropy (WPE)<sup>16</sup>.

As a test case, the present study focused on predicting participants' perceived pitch differences between two identical tones from neural irregularity. Computational modeling<sup>17</sup> as well as work on the auditory evoked potential<sup>18</sup> brought to bear the hypothesis that fluctuations in spontaneous neural activity are the most likely source for varying percepts in response to identical stimuli. Thus, if an individual reports perceptual differences for identical stimuli, these reports are likely influenced by the momentary or pre-stimulus degree of irregularity in the perceiver's neural system.

We demonstrate that the irregularity of the scalp EEG response, operationalized as pre-stimulus WPE, offers a clear relationship to spontaneous, pre-stimulus brain states as often described in terms of neural oscillatory power; to the sensory fidelity with which a stimulus is neurally encoded; and to the ensuing perceptual decision upon this stimulus. Moreover, entropy proves to be a sensitive marker for inter-individual, trait-like changes of neural irregularity that come with age.

## Results

Human participants of varying age ( $n = 19$ ; 19–74 years;  $49 \pm 18.75$  Median  $\pm$  Semi-Interquartile range, sIQR) were asked to indicate which one of two identical tones was higher in pitch. We were interested in (i) the influence of pre-stimulus irregularity in ongoing EEG activity on sensory encoding and the impending perceptual decision within individuals, as well as (ii) how these patterns of neural irregularity differ across individuals and change with age. Of note, entropy of the EEG signal was taken to quantify neural irregularity.

While participants were able to perform perceptual decisions on these physically identical tones and indeed did perceive pitch differences (see Supplementary Figures S1 and S2)<sup>17,19</sup>, decisions for the first tone being higher in pitch (S1, 57% on average) were overall slightly more frequent than for the second tone being higher in pitch (S2, 43% on average;  $13 \pm 4.5\% \pm$  SEM for the difference;  $t_{18} = 3.0$ ,  $p = 0.01$ ,  $r_e = 0.58$ ), representing a slight bias towards perceiving S1 as higher in pitch compared to S2.

**Patterns of irregularity in ongoing activity change with age.** We investigated both interindividual differences, or traits, as well as intraindividual variation, or states, in pre-stimulus entropy: First, we compared the variability of entropy in a pre-stimulus time-window ( $-0.4$  to  $-0.1$  s) across trials and participants using an Intraclass-correlation coefficient (ICC, ranging from 0 to 1, Fig. 1B, upper panel). The ICC allows us to quantify to which degree total variance is due to differences between participants.

As indicated by a fairly high Intraclass-correlation coefficient ( $ICC = 0.67$ )<sup>20</sup>, the sizable within-subject, trial-to-trial variability was in fact clustered at the level of participants (Fig. 1B). Thus, the variation in entropy values observed overall is attributable to both, state-like trial-by-trial fluctuation and trait-like between-subjects variation.

Exploring this between-subjects variation of entropy, we correlated participants' age with their individual pre-stimulus entropy averaged across trials (Fig. 1B, upper panel, inset), and their corresponding intra-individual variation (standard deviation; Fig. 1B, lower panel). Participants' age exhibited a high positive correlation with average pre-stimulus entropy ( $r = 0.73$ ,  $p = 0.0004$ ). This correlation, shown for electrode Cz in Fig. 1B, was significant at a large set of fronto-central and parietal electrodes (Fig. 1B, topography, highlighted electrodes  $p \leq 0.05$ ) but clustered towards central electrodes, forming a topography reminiscent of auditory evoked responses. Notably, the standard deviation of pre-stimulus entropy across trials was negatively correlated with age ( $r = -0.55$ ,  $p = 0.02$ , Fig. 1B, lower panel). Older participants thus exhibit increased levels of average pre-stimulus entropy, while at the same time showing decreased trial-to-trial variability of pre-stimulus entropy.

Note that when repeating both analyses based on mean entropy across the whole trial instead ( $-2$  to  $2$  s), the observed patterns were remarkably stable (Fig. 1C, see also Fig. S3). This underlines the robustness of the weighted permutation entropy measure against overly specific analysis choices when serving as a trait-like marker of neural irregularity.

**Irregularity of the EEG signal approximates 1/f noise.** To validate the increase of pre-stimulus entropy with age, we related it to an integrative measure of spectral shape, power spectral density (PSD): A fitted linear slope to the PSD is usually negative and reflects the inverse power-law dynamics of the human EEG<sup>8</sup>. Expectedly, individual PSD slopes became less negative with increasing participant age ( $r = 0.80$ ,  $p = 4 \times 10^{-5}$ ; Fig. 2A), with decreased power at low and increased power at higher frequencies, respectively. Notably, a similar effect could be substantiated when correlating age with the PSD slope derived from higher frequencies (30–60 Hz;  $r = 0.62$ ,  $p = 0.001$ ; Supplementary Fig. S4) recently suggested to capture changes in excitation–inhibition (E/I) balance<sup>21</sup>.

Since both average entropy and PSD slopes potentially capture a common underlying mechanism, the overall degree of irregularity, we correlated both measures and found a strikingly linear relationship ( $r = 0.84$ ,  $p = 8 \times 10^{-6}$ , Fig. 2B). Importantly, this relationship of the time-domain WPE measure and the spectral-domain PSD measure of neural irregularity retained a substantial effect size even after controlling for age ( $r = 0.61$ ,  $p = 0.006$ , Fig. 2B, inset). Additionally, entropy from a three-minute resting state recording that was carried out before the experiment started, was found to be almost as highly correlated with task entropy ( $r = 0.80$ ,  $p = 0.0004$ ) as was entropy from pre- and post-stimulus time periods ( $r = 0.99$ ,  $p = 10^{-6}$ , see Supplementary Fig. S3). This validates the utility of entropy and PSD slope as trait-like markers of interindividual variability in the time and frequency domain, respectively, of interest not only to aging research.

**Pre-stimulus irregularity captures low-frequency power and peri-stimulus phase alignment.** Previous work in non-human animals has characterized differences in synchrony and power of low-frequency oscillations that influence encoding and subsequent representations of stimuli<sup>10,11</sup>. Thus, we aimed to validate

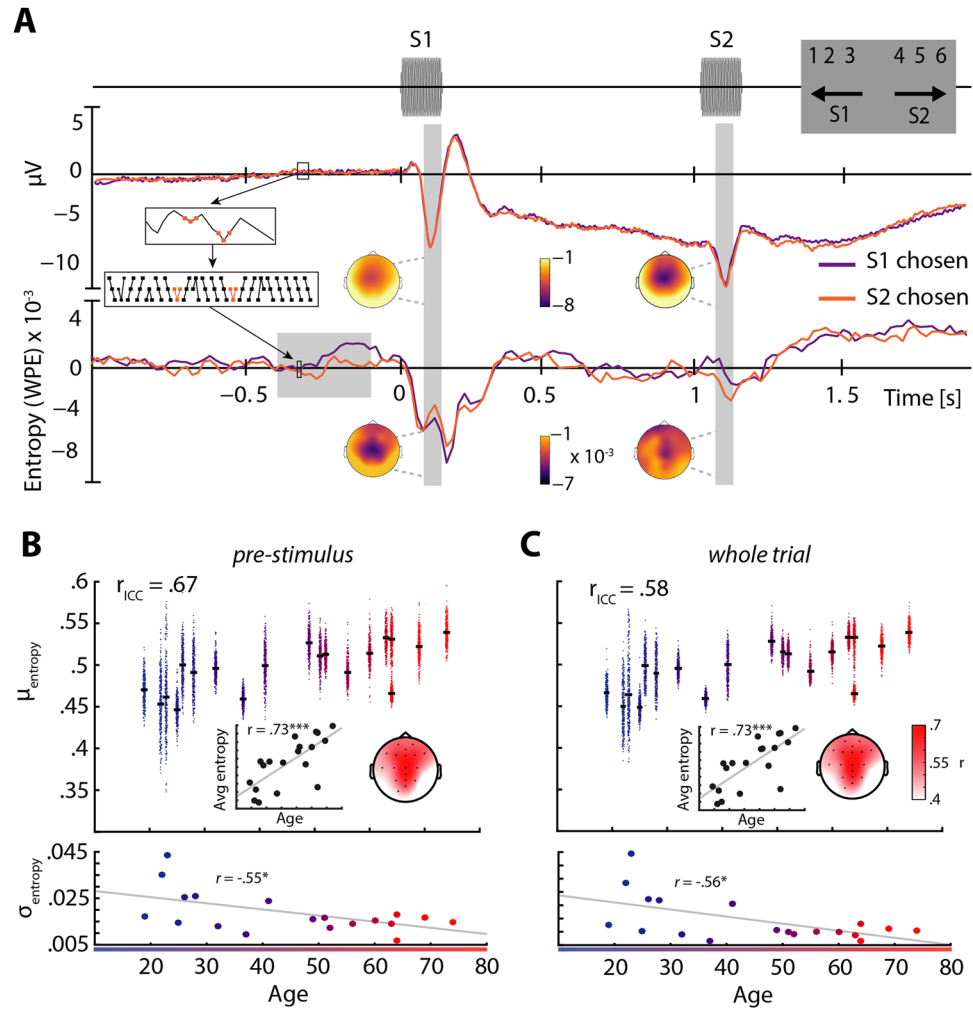


**Figure 1.** Trial structure, evoked responses, and entropy across age. **(A)** Trial structure and average responses. Two 650 Hz pure tones were presented separated by a fixed ISI of 900 ms and followed by the response screen (top panel). The middle panel shows the event-related potential (ERP) at electrode Cz (baseline  $-0.5$  to  $0$  s) for trials during which the first (S1, purple) versus the second tone (S2, orange) was perceived as higher in pitch. Topographies correspond to the N1 time-windows after S1 and S2 (grey areas). Colors show average microvolt values. Entropy (WPE) is computed by taking small snippets of voltage data, transforming them to rank sequences and computing the entropy of their frequency of occurrence. This procedure is illustrated in the small inset boxes that connect ERP and WPE representations. In the bottom panel, average WPE time courses of both conditions are shown (baselined relative to  $-1.5$  to  $-1$  s). Colors on topographies correspond to average WPE. **(B)** Pre-stimulus entropy (WPE) across age. Trial-wise averages of entropy in a pre-stimulus time window ( $-0.4$  to  $-0.1$  s, electrode Cz; grey shaded area) are shown as clouds of dots per subject (upper panel, warmer colors code higher age), black bars indicate average entropy across trials. Average entropy increased with age (upper panel, inset, electrode Cz), colors on topography correspond to average correlation coefficients  $r$ . The standard deviation of entropy values across trials decreased with age (lower panel). **(C)**, Same as B but for entropy data from whole trials (i.e.,  $-2$  to  $2$  s). \* $p < 0.05$ ; \*\*\* $p < 0.001$ .

pre-stimulus entropy as a measure of neural state by exploring its potency to also approximate fluctuations in low-frequency power and phase coherence of the human EEG.

To this end, we binned trials by baseline-corrected (whole trial) pre-stimulus entropy ( $-0.4$  to  $-0.1$  s) into four bins of equal trial number before calculating average power and inter-trial phase coherence (ITC) in each bin (see bar graphs in Fig. 3). Separately for each participant, we then fitted linear slopes to average power and IITC (logit-transformed ITC, see *Methods*), respectively, across the four bins of increasing pre-stimulus entropy. A cluster-based permutation test comparing slopes against zero revealed a broad negative cluster of decreasing oscillatory power with increasing entropy ( $-0.85$  to  $0.25$  s,  $1$ – $29$  Hz) displaying a fronto-central topography (Fig. 3A,  $p = 0.0009$ ,  $R = -0.71$ ). Notably, the same analysis for EEG power in higher frequencies ( $30$ – $70$  Hz) did not reveal any significant change across bins (all  $p > 0.05$ , Supplementary Fig. S5). Thus, pre-stimulus entropy tracked changes predominantly in low-frequency power, with lower power accompanying higher time-domain irregularity.

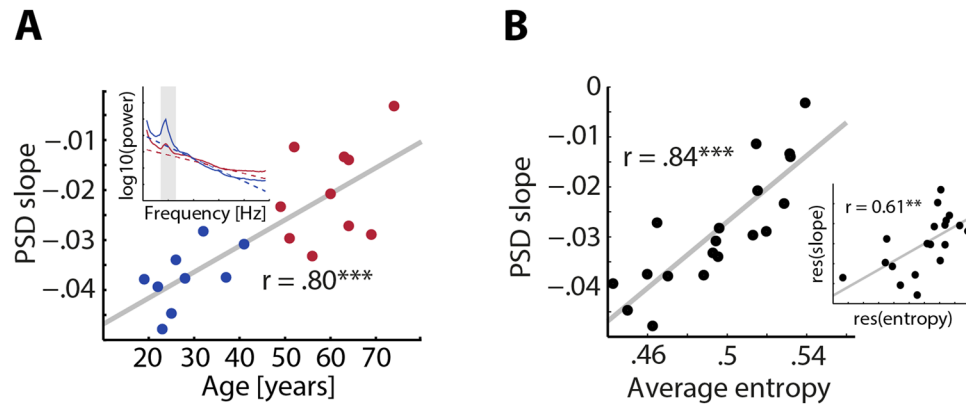


**Figure 2.** Weighted permutation entropy captures 1/f noise. **(A)** PSD slope changes with age. The slope of the PSD (inset) at electrode Cz over frequencies 1–30 Hz becomes less negative with increasing age. Younger subjects are shown in blue and older subjects in red. **(B)** WPE and PSD slopes are linearly related. The correlation of average entropy (WPE) and PSD slope is shown. The inset shows the same correlation after controlling statistically for participant age.  $**p < 0.01$ ;  $***p < 0.0001$ .

When analysing inter-trial phase coherence as a function of binned pre-stimulus entropy, a later, positive cluster ( $-0.25$  to  $0.30$  s,  $4$ – $12$  Hz) emerged around the onset of S1, indicating higher IITC with increasing levels of pre-stimulus entropy (Fig. 3B,  $p = 0.02$ ,  $R = 0.62$ ) over a set of frontal and central electrodes. Accordingly, with increasing signal irregularity prior to S1, the neural response to S1 in a theta-/alpha-band became more phase-coherent.

### Pre-stimulus irregularity and peri-stimulus theta-phase angle predict perceptual decisions.

Lastly, we explored the potency of our neural-irregularity measure, as well as the ensuing change in phase coherence during stimulus encoding, to explain the perceptual decisions based on the (physically identical) stimuli. Note in this context, that neither ERP amplitude nor oscillatory power predicted decisions (see Supplementary Fig. S6).

Sorting trials separately for each measure (electrode Cz, see *Predicting perceptual decisions* in the Methods section), we then analysed how the probability that a participant would choose the first tone as higher in pitch in a given trial would change, given this trial's pre-stimulus entropy on the one hand, or this trial's "phase similarity" at S1 onset ( $4$ – $6$  Hz, theta,  $0.01$ – $0.25$  s post S1 onset, electrode Cz). Phase similarity is a single-trial measure we derived based on the observed (across-trials) IITC effect. Phase similarity is calculated as the angular difference between a single trial phase at a given time and frequency (here: shortly after S1 in the theta frequency range) and the circular mean phase angle across trials. It thus captures how much a trial is deviating from the observed across-trials phase coherence in the time window of stimulus encoding.

Again, sorted trials were divided into four bins of equal trial number, where pre-stimulus entropy increased and angular distance from the mean angle decreased (i.e. IITC increased) with bin number (Fig. 4). Linear slopes fitted to the logit-transformed probability of choosing S1 across bins were significantly positive for both pre-stimulus entropy ( $t_{18} = 3.15$ ,  $p = 0.006$ ,  $r_e = 0.60$ ) and angular distance from the mean ( $t_{18} = 3.20$ ,  $p = 0.005$ ,  $r_e = 0.60$ ). Importantly, this effect did not qualitatively change when three, five, or six bins were used (see Supplementary Fig. S5) and thus appeared independent of bin number. Note that sorting for pre-stimulus low frequency power did not result in significantly positive slopes ( $t_{18} = 1.7$ ,  $p = 0.1$ ,  $r_e = 0.38$ ; Supplementary Fig. S6). Hence, a participant was more likely to perceive and decide on the first tone as higher in pitch if this first tone was presented in a period of relatively high neural irregularity. On the other hand, a participant showed a higher probability of perceiving, and deciding for the first tone as higher in pitch if the theta phase angle on that trial was more similar to the average theta-phase angle across trials.

## Discussion

With decreasing amounts of sensory information to base a perceptual decision on, the impact of spontaneous variations in brain activity is growing. Thus, in the complete absence of sensory evidence, fluctuations in the states of the brain, including the irregularity of neural activity, should be driving the perceptual decision. At the same time, such neural irregularity might be key to delineate neural changes that come with age. Here, we thus tested the potency of irregularity in the human EEG to describe both neural traits and states by (i) tracking age related changes in ongoing brain activity and (ii) by predicting discriminative decisions between two identical tones. Entropy of the EEG signal was employed as a time-resolved quantification of neural irregularity. Results can be summarized as follows: First, average irregularity of the EEG signal increased with age, paralleled by a reduction in variability. Second, individual pre-stimulus irregularity did not only capture low-frequency oscillatory power and influenced the encoding fidelity of presented tones but also biased perceptual decisions.

Aging has been shown to manifest in the brain signal by lower temporal variability of hemodynamic activity<sup>22</sup> and changes to the power spectrum of the EEG<sup>23</sup>, both possibly describe consequences of structural and functional dedifferentiation. But how does irregularity of the EEG signal relate to aging and the established markers of changing activity patterns?

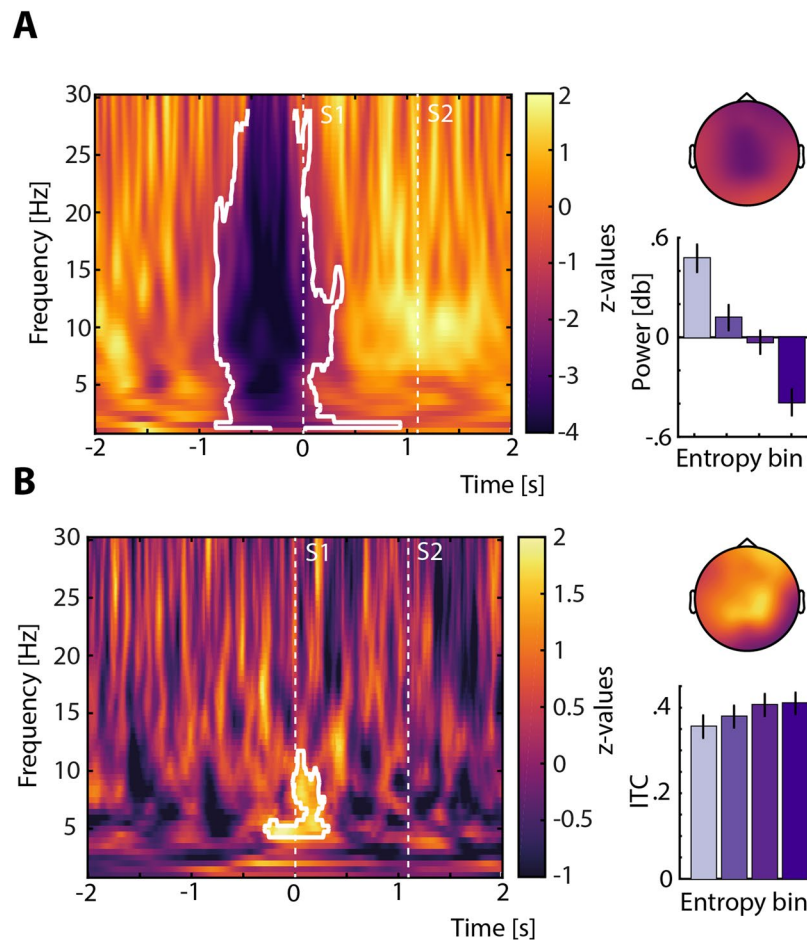


**Figure 3.** Time–frequency patterns of oscillatory power and phase coherence as a function of pre-stimulus entropy. **(A)** Pre-stimulus power decreases with increasing entropy. Oscillatory power between 1 and 29 Hz significantly decreased with increasing pre-stimulus WPE. Colors indicate z-values resulting from a cluster-based permutation dependent samples t-test that compared slopes of linear trends across four bins of oscillatory power against zero, which were derived by sorting for increasing pre-stimulus entropy. The resulting negative cluster ( $p = 0.0009$ ) is outlined in white and revealed a fronto-central topography. The bar graph shows average power within the cluster per bin ( $\pm 1$  between-subject standard error of the mean, SEM). Darker colors correspond to higher pre-stimulus entropy. **(B)**, Low-frequency (theta) phase-coherence at S1 increases with entropy. ITC around the onset of S1 increased with pre-stimulus entropy. Colors again indicate z-values from a similar cluster-based test as outlined for power, testing linear slopes across four bins of ITC against zero. One positive cluster around S1 onset ( $-0.25$  to  $0.30$  s, 4–12 Hz) with a predominantly central and frontal topography was found ( $p = 0.02$ ) and is outlined in white. The bar graph shows average ITC within the positive cluster per bin ( $\pm 1$  SEM). Darker colors in the bar graphs correspond to higher pre-stimulus entropy.

Strikingly, the observed age-related increase of irregularity was accompanied by a decrease in the variability of EEG irregularity across trials (Fig. 1B). Note that this effect was not linked to previously observed age-related alterations in amplitude and latency of evoked responses<sup>24,25</sup>, since it was equally present both in pre-stimulus and whole-trial time windows (see Fig. 1B and C). Beyond replicating and extending results that reported age-related increases in neural irregularity<sup>7,8</sup>, these results offer a clear marker of aging in the EEG signal and close an important gap: they allow us to link electrophysiology to findings from fMRI research that emphasized reduced trial-to-trial brain signal variability with increasing age<sup>5,6</sup>.

Further validating our results, older participants showed shallower power spectral density (PSD) slopes. Both measures, entropy and PSD slope, are likely tracking the described twofold shift in the power spectrum that is also referred to as increased  $1/f$  noise<sup>8</sup>. This, alongside the absence of ERP differences between age groups, renders it likely that the observed increase in entropy is in fact a time-domain reflection of a relative enhancement in higher-frequency noise and/or a reduction in power at lower frequencies. This interpretation gains further support from a comparison of weighted permutation entropy as used here with multiscale entropy approaches (Supplementary Fig. S7)<sup>26,27</sup>.

If so, which structural and functional changes mediate these age-related alterations in brain signal variability and  $1/f$  noise? During aging, the loss in number of neurons is negligible<sup>28</sup>, especially compared to the age-accompanying damage of white matter integrity<sup>29</sup>, which among other modifications is responsible for a

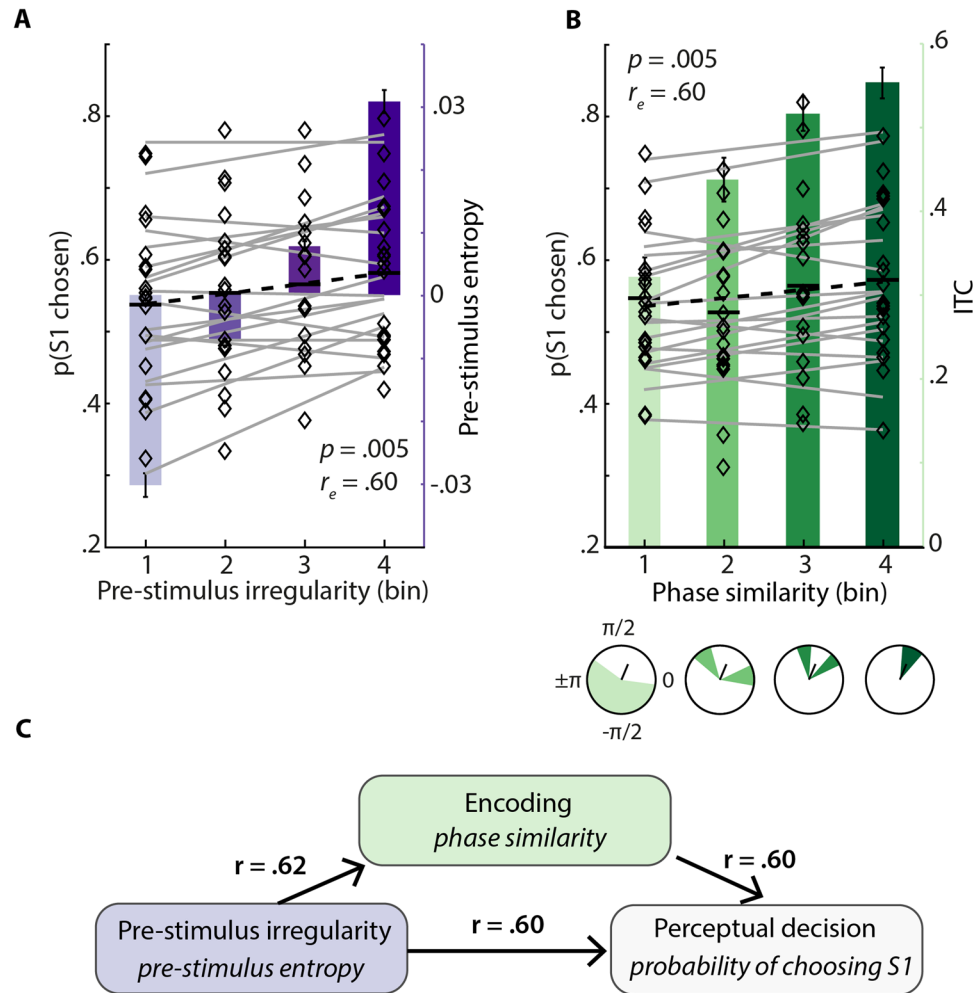


**Figure 4.** Pre-stimulus entropy and theta (4–6 Hz) phase angle at sensory encoding both predict perceptual decisions. **(A)** The probability of choosing S1 is shown for each subject and entropy bin (diamonds). Grey lines depict single-subject slopes fitted to probabilities across bins for visualization. Slopes were significantly positive on average (black dashed line,  $p = 0.005$ ) representing an increase of choices for S1 with increasing pre-stimulus entropy (represented by bars of darkening lilac  $\pm 1$  SEM). **(B)** Again probabilities of choosing S1 are shown per participant and bin together with grey lines representing slopes. Here, with increasing bin number, theta phase similarity at S1 onset increased, hence, ITC increased (bars of darkening green  $\pm 1$  SEM). With increasing phase similarity, decisions for S1 got more likely (black dashed line,  $p = 0.005$ ). Circle plots show distributions of phase angles per bins for an exemplary participant along with the mean angle across trials. **(C)** Links of irregularity, encoding and decisions. The found relations of pre-stimulus irregularity with encoding and perceptual decisions as well as the link of encoding and perceptual decisions are visualized. Arrows imply temporally ordered, not strictly causal connections. Note that  $r$  denotes the observed effect size. Colors correspond to measures as visualized in **(A)** and **(B)**.

decline of large-scale structural networks. Importantly, the connectivity of higher-order as well as sensory functional networks shrinks with age<sup>30,31</sup>. A shallower power spectrum thus might not only reflect increased 1/f noise<sup>8,23</sup> but also a decreased utilization of long-range neural networks<sup>32,33</sup> and a parallel increase in local processing<sup>7</sup>. Increased irregularity in older brains during an auditory discrimination task therefore, by proxy, also points towards reduced connectivity in functional networks. Furthermore, decreased trial-to-trial variability might trace back to reduced spatial variations of brain activity that have been shown to come with age<sup>6</sup>.

Additionally, age-related changes in the slope of power spectra over higher frequencies (30–60 Hz; Supplementary Fig. S4) have recently been hypothesized to dynamically track changes in the excitation-inhibition (E/I) balance via a positive relationship between PSD slopes and E/I ratio<sup>21</sup>. Older brains thus might show increased E/I ratios as compared to younger ones (for results from the auditory domain see e.g. refs<sup>34–36</sup>). If that is the case, irregularity of the EEG possibly captures global inter-individual changes in the brain signal, that is, it describes age-related change as a neural trait. By design and as outlined in more detail below, but unlike PSD, entropy additionally offers information regarding ongoing activity on a trial-wise, time-resolved basis and thus allows estimating neural states.

Non-human animal physiology research on the neural dynamics of sensory processing has recognized low-frequency power as a proxy of synchronized and desynchronized neural states in ongoing cortical activity<sup>10,11,37</sup>. Periods of relatively low power indicate desynchronized states. A sensitive (and potentially more versatile) measure of neural irregularity or desynchronization should thus transfer these findings to the human brain and exhibit a negative relationship with low-frequency power. Notably, spontaneous variations in oscillatory power have also been linked to perceptual processes in humans<sup>38,39</sup>. Here, with higher irregularity prior to stimulus onset, power in low frequencies decreased. Although the frequency range may seem rather broad, decreases were strongest between 1 and 20 Hz, a frequency range previously used as a proxy for neural state<sup>11</sup>.

The fronto-central topography of oscillatory power decreases appears compatible with auditory cortical generators and thus represents growing evidence for an impact of pre-stimulus neural state on the processing of sensory information. Unifying results from different methodologies and species, the entropy measure used in the present study (WPE) thus offers a new and promising approximation of irregularity in neural activity and thereby quantifies the degree of desynchronization in the human EEG.

Importantly, increasing pre-stimulus irregularity additionally was associated with higher phase coherence during the period of stimulus encoding. This observation aligns well with recent results from non-human animal work that related stronger desynchronization of ongoing activity to lower variability of neural responses to sensory stimulation<sup>40</sup>.

Furthermore, although a dependence of sensory encoding and cortical representations on the degree of neural irregularity has been noted before<sup>10,11,37</sup>, this relationship has not yet been revealed for humans. Neurally encoding the same stimulus in a more desynchronized state of cortical activity should lead to a more thorough sensory representation<sup>10</sup>. The present data propose that pre-stimulus irregularity influences the encoding and subsequent representation of the first tone (S1), resulting in a higher-fidelity representation of S1 compared to S2.

When comparing two physically identical tones, the tone that is neurally encoded more thoroughly should be more likely to be decided on, due to a higher fidelity or saliency with which it was encoded (Fig. 4). The next section will discuss this in more detail.

Decisions in the face of perceptual ambiguity are known to be influenced by pre-stimulus patterns in low-frequency power and phase of oscillations in the human EEG<sup>41–43</sup>. The impact of irregularity in ongoing activity on perceptual processes and decisions, however remains unknown. In addition to irregularity-driven changes in encoding, we find that with neural irregularity prior to S1 onset, S1 became more likely to be chosen as higher in pitch (Fig. 4A). Although a reversed effect could have been expected for S2 (i.e. higher irregularity prior to S2, higher probability of decisions for S2 as being higher in pitch), only a slight trend was found (13 negative slopes as compared to 4 negative slopes when sorting for pre-S1 entropy,  $p = 0.23$ ). We deem it most likely that the comparably short ISIs after S1 precluded a full reversal of entropy and according IITC around S2, a matter well described for auditory evoked potentials<sup>44,45</sup>. Note that in these analyses we focused solely on intra-individual variations, accordingly comparing states as opposed to traits. Since the degree of irregularity in the EEG signal approximated the neural state of ongoing activity in terms of pre-stimulus desynchronization, we take this as evidence of the neural state influencing perceptual decisions. Thus, pre-stimulus irregularity state influences pending decisions, likely by changing response bias<sup>46</sup>.

In addition, however, pre-stimulus neural irregularity also shaped neural encoding of to be judged stimuli, as evidenced by our ITC analysis (Fig. 3). We would thus expect that this increased sensory-encoding strength should also be directly predictive of perceptual decisions. Indeed, with increasing theta phase similarity at S1 onset, which can be thought of as a measure of optimized encoding, the probability that S1 was chosen also increased (Fig. 4B). This suggests an additional influence of the fidelity of early sensory representations on perceptual decisions (compare Fig. 4A and B). Again, a more thorough encoding of the first tone should lead to a more detailed and hence more salient sensory representation, which then gets chosen at the end of the trial. If this is the case, saliency of different representations should be of prime importance for a perceptual decision — and not the exact stimulus feature regarding which two stimuli are compared. Hence, we predict qualitatively similar results if the relevant stimulus dimension were to be changed (e.g. if listeners judged duration instead of pitch; see ref<sup>18</sup> for a similar approach).

The present data propose that states of pre-stimulus irregularity influence perceptual decisions via changes to neural encoding, which in turn impacts the decision via modulating the salience of representations (cf. Fig. 4C). We hereby expand research on the influence of spontaneous variations in brain activity on perceptual decisions in two different ways: First, we establish a trial-wise measure of irregularity in ongoing brain activity as compared to most studies of the field that relied on averaged activity estimates<sup>47,48</sup> (e.g. Hesselmann *et al.*<sup>47</sup>; Amitay *et al.*<sup>48</sup>). Second, we here show trial-wise irregularity of spontaneous brain activity to indeed predict both the encoding of presented tones and the ensuing perceptual decision that follows at the end of each trial, as had been previously implied<sup>17,18</sup>.

In sum, neural irregularity not only characterizes behaviourally relevant brain states, but also captures trait-like changes to individual neural dynamics as they come with age.

## Materials and Methods

**Participants.** Nineteen healthy participants (19–74 years; Median age  $49 \pm 18.75$  sIQR, 12 female) with self-reported normal hearing took part in the experiment. Participants gave written informed consent and were financially compensated. None of the participants reported a history of neurological or otological disease. The study was approved by the local ethics committee of the University of Lübeck and all experimental procedures were carried out in accordance with the registered protocol.

**Stimulus material.** One 650-Hz, 150-ms pure tone (sampled at 44.1 KHz, rise and fall times of 10 ms) was generated using custom MATLAB<sup>®</sup> code (R2014b; MathWorks, Inc., Natick, MA). In each trial during the main experiment, this pure tone was presented twice (i.e., as a pair) with an inter-stimulus-interval (ISI) of 900 ms

using Sennheiser® HD-25-I headphones. To ensure accurate timing, auditory stimuli were presented via the Psychophysics toolbox<sup>49</sup> and an external low-latency audio interface (Native Instruments, Berlin, Germany). Note that the tone pairs were presented perfectly audible (i.e., no masking noise) at a comfortable loudness level, which participants could adjust themselves during practice trials.

**General procedure.** Participants were seated in a quiet room in front of a computer screen. First, after 20 practice trials, they underwent an adaptive tracking procedure that resembled the main experiment but consisted of pairs of different tones which gradually were rendered more similar (see supplementary methods). Subsequently, they performed the main task, which consisted of identical stimuli only before carrying out a second run of the adaptive tracking procedure. In all parts of this study (practice trials, adaptive tracking, main experiment), participants had the task to decide on each trial which one of the two tones was higher in pitch.

**2AFC pitch discrimination task with confidence judgement.** Subjects were instructed to indicate after each pair of presented pure tones, which one was higher in pitch by pressing one button on the computer keyboard. They were encouraged to include their confidence and hence the degree to which the respective tone was perceived as higher in pitch by using a rating between 1 and 6 (Fig. 1). Here, a rating of 1 corresponded to the perception of “the first tone being clearly higher in pitch” and a rating of 6 to “the second tone being clearly higher in pitch”. The mapping of response buttons was reversed for approximately half of the subject sample (9 of 19 subjects, in random order).

A first 150-ms tone (S1) was followed by a fixed 900-ms silent interval before the second 150-ms tone (S2) was presented. Subsequently, the response screen was shown until subjects entered their response with a limit of 2 s (Fig. 1). A grey fixation cross was presented throughout the trial and subjects were instructed to fixate their vision on it at all times. All visual content was presented and responses were recorded using custom MATLAB® scripts and the Cogent 2000 toolbox.

After an inter-trial-interval, randomly jittered between 2 and 4 s, the next trial started, indicated by the fixation cross changing its color from grey to light green and back to grey within 500 ms. The experiment consisted of a total of 500 trials, divided over five blocks of 100 trials each. The first trial of each block was started by the participants as soon as the experimenter had left the room. Blocks were separated by short breaks. The experiment took about 60 minutes in total.

Bogus feedback was provided after each of the first 20 trials in every block, where, in 65% of all feedback trials, a positive feedback indicating a correct pitch discrimination was given. This proportion of positive bogus-feedback was chosen to keep participants engaged in the task and took into account a comparable previous research design<sup>18</sup>. In the case of trials involving auditory bogus feedback, the response screen was followed by a sound indicating correct or incorrect answers after 100 ms. Additionally, after every 20th trial, sham accuracy scores representing average performance in the past 20 trials, randomly chosen from a uniform [55;65]-% distribution were displayed on the screen for 3 s. Note that, for further analyses, all trials followed by feedback were excluded.

After the experiment, subjects frequently reported that they perceived pronounced pitch differences between the two (physically identical) tones. Before debriefing, no subject raised concerns regarding the actual nature of the stimuli. In fact, behavioural pilot experiments ( $n = 10$ ) showed that even participants who knew that a high proportion of all trials would contain identical stimuli still reported to perceive considerable differences in pitch. In combination with previous experimental work that used identical stimuli in a comparable task structure<sup>18,19,48</sup> we are thus confident that participants paid attention to the task and engaged in it. Additionally, a computational modelling study that estimated the magnitude of perceived differences in similar tasks as pronounced as 8.5 Hz in 50% of all trials and larger than 20 Hz in 10% of all trials<sup>17</sup> supports the feasibility of such a task structure.

**Behavioural data analysis.** As expected with physically identical stimuli, only few participants exhaustively used the full range of “first vs. second tone had higher pitch” ratings (1–6). Most ratings were instead centered on the middle range (3–4) of possible ratings. The variance of responses over trials showed no correlation with participant age ( $r = -0.07$ ,  $p = 0.78$ ). We thus binarized the rating responses and coded ratings 1–3 as “first stimulus chosen as higher in pitch” and ratings 4–6 as “second stimulus chosen as higher in pitch”. Proportions of both binarized response types were logit-transformed (see *EEG time- and frequency domain analyses*) prior to statistical analysis to approximate normality for the originally [0;1]-bound proportions. To check for response bias (i.e. favouring one choice over the other), these transformed proportions were compared using a paired t-test. We additionally tested for and ruled out the presence of more complex response strategies by testing for patterns of autocorrelated responses (see Supplementary Methods and Fig. S1).

**EEG recording and preprocessing.** EEG was recorded with a 24-channel mobile EEG setup (SMARTING, mBrainTrain, Belgrade, Serbia) at a sampling rate of 500 Hz, a resolution of 24 bits and a bandwidth of DC–250 Hz. Electrode impedances were kept below 10 k $\Omega$ . The amplifier was attached to the EEG cap (Easycap, Herrsching, Germany). Recordings were online referenced to electrode FCz and grounded to electrode AFz. All data and event-related triggers were transmitted to a nearby computer via Bluetooth where both were saved using the Labrecorder software, which is part of the Lab Streaming Layer (LSL)<sup>50</sup>.

Offline, continuous data were bandpass filtered from 0.5 Hz (–12 dB attenuation at 0.03 Hz) to 100 Hz (–12 dB attenuation at 100.2 Hz) with a zero-phase finite impulse response filter (filter order 1200). Filtering and all other analysis steps were carried out in MATLAB® 2014b using custom scripts and the fieldtrip toolbox<sup>51</sup>. After re-referencing to average mastoids, we epoched the data from –2 s to +2 s around onset of S1. The first 20 epochs of every block were excluded from further analysis since they involved feedback. An independent component analysis was carried out and components related to eye-movements, muscle activity or heartbeat were identified and removed from the data on the basis of their time-courses, frequency spectra and topographies. Subsequently,

remaining artefactual epochs were removed after visual inspection. On average, 43% ( $\pm 12\%$  SD) of components and 7% ( $\pm 4\%$  SD) of trials were removed. Importantly, the number of removed components was not correlated with participants' age ( $r = 0.08$ ,  $p = 0.76$ ) or average entropy ( $r = 0.25$ ,  $p = 0.30$ ).

**Information theoretic measure.** Entropy is taken to quantify the information contained in a signal. Accordingly, a variety of entropy-based measures such as Shannon Entropy<sup>52</sup>, Kolmogorov-Sinai Entropy<sup>53</sup>, Approximate Entropy<sup>54</sup> or Sample Entropy<sup>55</sup> has been suggested and has been used to estimate the complexity of natural time series data. Each of them however is constrained by required metric properties of the input data. In contrast, Permutation Entropy (PE) is a form of symbolic or rank-based entropy measure<sup>56</sup> that estimates the complexity of a time series while being robust against various degrees of non-linearity in the signal. Furthermore, PE takes into account the temporal structure of a signal and is computationally very efficient<sup>57</sup>. Permutation entropy is thus particularly attractive as an entropy measure for biological time-series as obtained with EEG, since these incorporate non-linear processes at least to some degree. Although a full introduction on the principles of entropy calculation is beyond the scope of this article, the basic rationale of PE (and, as used here, a weighted version of PE; WPE) shall be outlined briefly below.

The basic calculation of PE can be split up in three steps: First, data are divided into overlapping windows of reasonable size (e.g. 50 samples, but see Staniek and Lehnertz<sup>58</sup> for an overview of parameter selection for PE). Second, the time series data within the windows are mapped into symbolic space by dividing each window into short sub-sequences (e.g. 3–5 samples size, 1 sample distance) and calculating their ranks, resulting in so called motifs. Importantly, the number of different motifs that can occur is determined by the number of samples in one sub-sequence (motif length). Using a motif length of 3 for example results in  $3! = 6$  possible motifs. Third, the occurrences of each motif within each bigger time window are counted and their frequency of occurrence is used to calculate one Shannon Entropy value for each motif. These values finally are added before being multiplied with  $-1$  to arrive at the PE of one window. Given a sufficiently high sampling frequency (i.e., if the number of samples within a window allows all possible motifs to occur more than once), PE can be calculated with high precision, still offering satisfying time resolution.

The defining feature of PE as compared to other entropy algorithms is that the calculation of PE is not based on the real values of the time series but on sequences of ranks, the so-called motifs. While this makes PE very robust against outliers and suitable for non-linear time-series, it disregards, by design, all metric information in a given data window. For example two windows containing the voltage ( $\mu\text{V}$ ) measurements  $[-1, +1, +4]$  and  $[-20, +60, +150]$  would be mapped onto the same motif (1, 2, 3). To overcome this potential limitation, Fadlallah and colleagues<sup>16</sup> proposed a weighting of occurrence frequencies that enter PE calculation: The relative frequency of occurrence of every motif is weighted by the variance of the data segments from which this motif was derived, so that its contribution to the resulting Weighted Permutation Entropy (WPE) is increased for increasing variance. Importantly, this does not imply that the metric information that was willingly excluded before, is fully reintroduced but rather that relative variance is used as an additional source of information to improve the sensitivity of the measure. As a result, WPE retains all features of PE but is more sensitive to abrupt changes in a signal as revealed by the application to both synthetic noisy time series and EEG data<sup>16</sup>.

We calculated WPE (in the following and above referred to as entropy) following the same procedure as outlined above for the extraction of PE time courses: For each electrode and trial, entropy was computed using a sliding window of 50 samples (corresponding to 100 ms in the present data) that was shifted in steps of 10 samples (20 ms), a motif length of 3 and a time delay factor of 1. This resulted in entropy time-courses of 200 samples per trial.

To explore the impact of pre-stimulus entropy on low-frequency power fluctuations, encoding and perception of the presented tones, trials were sorted for increasing baseline-corrected pre-stimulus entropy (averaged over the interval from  $-0.4$  to  $-0.1$  s at electrode Cz). Subsequently, sorted trials were separated into four equally sized, non-overlapping bins (number of trials/4) resulting in two grouping variables per trial: the given response and the bin membership, whereas for the latter higher values corresponded to higher levels of pre-stimulus neural irregularity.

**EEG-irregularity as an inter-individual marker of aging.** To compare the degree of irregularity between participants of different age, entropy at every electrode was averaged per subject over all trials and subsequently correlated with age. Since trial-wise averages of entropy did not only display considerable inter- but also intra-individual variance, which appeared to shrink with increasing age (see Fig. 1B), we calculated the intraclass correlation coefficient (ICC). Note that the relationship of entropy and age was strikingly unaffected by different time-windows that were used for averaging before correlating averages with age (Fig. 1B, but see Supplementary Fig. S3). Since our primary interest lay in the irregularity patterns of ongoing activity, we used pre-stimulus entropy for all further analysis.

To relate the fairly recent measure of entropy to other, commonly suggested measures of neural irregularity<sup>8,23</sup>, we also calculated the power spectral density (PSD) from subjects' trial data using 2-s-windows (which overlapped by 50%, yielding three PSD estimates per trial that subsequently were averaged). An individual linear fit across frequencies between 1 and 30 Hz (excluding the 8–13-Hz alpha range)<sup>8</sup> was obtained for the resulting PSD estimate. The slope of the resulting line can be used to estimate the degree of  $1/f$  noise in the power spectrum<sup>59,60</sup>. In brief, a more uniform distribution of neural oscillatory power across frequencies (i.e., a shallower spectrum) is indicative of increasing neural irregularity. We thus expected flatter spectra and accordingly more positive regression slopes for older compared with younger participants. To test this, we calculated the Pearson correlation of age and the slope of the linear regression line fitted to the power spectrum.

**Basic EEG time- and time-frequency domain analyses.** EEG data were separated into trials for which a response indicating the first versus second tone as higher in pitch was made. Time-locked averages (i.e., event-related potentials, ERPs) were computed for every participant and condition (S1 higher vs. S2 higher) separately.

To assess potential differences in ERP amplitude on the group level, we performed a cluster-based permutation dependent samples t-test<sup>61</sup>, comparing the ERP in trials where the first versus the second tone was later chosen as higher in pitch. This test proceeds by first clustering adjacent bins with t-values with  $p < 0.05$  in electrode–time space, where a cluster consisted of at least three neighbouring electrodes. The sum of all t-values in a cluster subsequently was compared against the distribution of 10,000 random clusters, which were generated by iteratively permuting the labels of conditions. The resulting p-value of a cluster corresponds to the proportion of performed Monte Carlo iterations that exceed the summed t-values of the empirically observed cluster.<sup>61,62</sup>

Complex-valued time–frequency Fourier representations of the data were obtained by means of convoluting single-trial time courses with frequency-adaptive Hann-tapers of 4 cycles width. Oscillatory power from 1 to 30 Hz (in 0.5 Hz steps) and from 30 to 100 Hz (2 Hz steps) was obtained by squaring the modulus of the Fourier spectrum. The average power estimate across trials was then baseline corrected and represented as change in Decibel (dB) relative to the mean power during a  $[-2; -1]$  s pre-stimulus time-window. Note that this procedure was performed separately for each of the four bins that resulted from sorting for pre-stimulus entropy as outlined above. To relate average oscillatory power to the pre-stimulus state of the brain (i.e. the level of irregularity), we performed a subject-wise linear fit across all bins, separately for every electrode, time-point and frequency. The resulting slope qualifies the relationship of pre-stimulus irregularity and oscillatory power. Slopes were tested against zero using the same cluster-based approach outlined above for time-domain data.

**Inter-trial phase coherence (ITC).** We then calculated Inter-trial phase coherence (ITC;  $0 \leq \text{ITC} \leq 1$ ) for every bin of sorted trials to test for differences in phase coherence between different levels of pre-stimulus neural irregularity. Note that ITC can also be expressed as  $1 - \text{circular variance}$  (e.g. Breakspear *et al.*<sup>63</sup>), where high ITC values reflect relatively low levels of variance in the precise phase angle across trials at a given time (e.g. stimulus onset) and frequency. Thus, ITC poses an across-trials proxy for the variability of phase angles. Since measures of phase coherence are strongly influenced by the number of trials on which they are computed<sup>64</sup> we used the same number of trials for each participant from four levels of pre-stimulus irregularity (see *Information-theoretic measure*) to calculate ITC and power estimates. For further metric and statistical analysis, the  $[0;1]$ -bound ITC measure at every electrode  $e$ , time-point  $t$  and frequency  $f$  was logit-transformed, an approach previously shown to outperform other transformation techniques for binomial and proportional data<sup>65</sup>. This resulted in a  $[-\infty; +\infty]$ -bound measure of

$$\text{lITC}_{e,t,f} = \ln \left( \frac{\text{ITC}_{e,t,f}}{1 - \text{ITC}_{e,t,f}} \right)$$

To analyse how pre-stimulus irregularity influences phase-coherent responses to the first tone, for each subject, linear fits across the four lITC estimates were performed per electrode, time-point and frequency as described above for average oscillatory power. Here, slopes approximate the relation of pre-stimulus entropy and the consistency of phase angles in response to a stimulus and were tested against zero using the same cluster-based approach outlined above.

**Predicting perceptual decisions.** As outlined above, trials were sorted ascendingly for pre-stimulus entropy as a marker of irregularity in the EEG-signal before stimulation onset. Importantly, we did not only expect pre-stimulus irregularity to impact the encoding of presented stimuli but ultimately to affect pitch perception and thereby the impending decision. The sorting of trials for pre-stimulus entropy thus also was used to establish bins of behavioural responses.

Additionally to the influence of pre-stimulus state on encoding that was revealed by a positive cluster around stimulus onset (Fig. 2), the encoding of a tone and the ensuing decision might have been influenced by variations in evoked responses unrelated to spontaneous changes in the pre-stimulus state. Thus, for every trial, the phase angle at the central point of the found cluster (4–6 Hz, 0.01–0.25 s, electrode Cz) was extracted and compared to the corresponding average phase angle across trials by computing the absolute angular distance, resulting in “phase similarity”. The result, one value of phase similarity per trial, captures the trial-wise difference in phase from the stereotypic response during encoding. Subsequently and analogous to the approach used for pre-stimulus entropy, trials were sorted for increasing phase similarity and split up into four non-overlapping bins of equal trial number. Hence, to the existing grouping variables (response, entropy bin) per trial, another one, phase similarity bin membership, was added. Note that phase-angles were more similar to the average phase with increasing bin-number and hence ITC can be expected to increase with bin-number.

To quantify the impact of pre-stimulus irregularity and evoked responses on the ensuing perceptual decision, the probability of perceiving the first tone as being higher in pitch was calculated for each participant and bin before undergoing logit transformation. Per subject and binning variable (entropy / phase similarity), a first order polynomial was fitted to the logit-transformed probabilities across all four bins. The resulting slopes were tested against zero using a one-sample t-test.

**Effect sizes.** As a measure of effect size for t-statistics resulting from both dependent- and independent-sample t-tests, we calculated the  $r_{\text{equivalent}}$ <sup>66</sup> henceforth denoted as  $r_e$ . For multiple comparisons, e.g. when comparing electrode  $\times$  frequency  $\times$  time pairs, we averaged effect sizes of all t-tests within a significant cluster to estimate  $R_e$ <sup>42,62</sup>.

**Data availability.** The datasets generated and analysed during the current study are available from the corresponding author on reasonable request.

## References

- Faisal, A. A., Selen, L. P. J. & Wolpert, D. M. Noise in the nervous system. *Nat. Rev. Neurosci.* **9**, 292–303 (2008).
- Arieli, A., Sterkin, A., Grinvald, A. & Aertsen, A. Dynamics of ongoing activity: explanation of the large variability in evoked cortical responses. *Science* **273**, 1868–1871 (1996).
- Arazi, A., Censor, N. & Dinstejn, I. Neural Variability Quenching Predicts Individual Perceptual Abilities. *J. Neurosci.* **37**, 97–109 (2017).
- Dinstejn, I., Heeger, D. J. & Behrmann, M. Neural variability: friend or foe? *Trends Cogn. Sci.* **19**, 322–328 (2015).
- Grady, C. L. & Garrett, D. D. Understanding variability in the BOLD signal and why it matters for aging. *Brain Imaging and Behavior* **8**, 274–283 (2014).
- Garrett, D. D., Kovacevic, N., McIntosh, A. R. & Grady, C. L. The modulation of BOLD variability between cognitive states varies by age and processing speed. *Cereb. Cortex* **23**, 684–693 (2013).
- Sleimen-Malkoun, R. *et al.* Brain Dynamics of Aging: Multiscale Variability of EEG Signals at Rest and during an Auditory Oddball Task. *eNeuro* **2**. *ENEURO*. **0067-14**, 2015 (2015).
- Voytek, B. *et al.* Age-Related Changes in 1/f Neural Electrophysiological Noise. *J. Neurosci.* **35**, 13257–13265 (2015).
- Garrett, D. D. & Kovacevic, N., McIntosh, a. R. & Grady, C. L. Blood Oxygen Level-Dependent Signal Variability Is More than Just Noise. *J. Neurosci.* **30**, 4914–4921 (2010).
- Marguet, S. L. & Harris, K. D. State-Dependent Representation of Amplitude-Modulated Noise Stimuli in Rat Auditory Cortex. *J. Neurosci.* **31**, 6414–6420 (2011).
- Pachitariu, M., Lyamzin, D. R. & Sahani, M. & Lesica, N. a. *State-dependent population coding in primary auditory cortex.* *J. Neurosci.* **35**, 2058–73 (2015).
- Nicolaou, N. & Georgiou, J. Detection of epileptic electroencephalogram based on Permutation Entropy and Support Vector Machines. *Expert Syst. Appl.* **39**, 202–209 (2012).
- Dickten, H., Porz, S., Elger, C. E. & Lehnertz, K. Weighted and directed interactions in evolving large-scale epileptic brain networks. *Sci. Rep.* **6**, 34824 (2016).
- Bruzzo, A. A. *et al.* Permutation entropy to detect vigilance changes and preictal states from scalp EEG in epileptic patients. A preliminary study. *Neurol. Sci.* **29**, 3–9 (2008).
- O’Hora, D. *et al.* Age-related task sensitivity of frontal EEG entropy during encoding predicts retrieval. *Brain Topogr.* **26**, 547–557 (2013).
- Fadlallah, B., Chen, B., Keil, A. & Príncipe, J. Weighted-permutation entropy: A complexity measure for time series incorporating amplitude information. *Phys. Rev. E* **87**, 22911 (2013).
- Micheyl, C., McDermott, J. H. & Oxenham, A. J. Sensory noise explains auditory frequency discrimination learning induced by training with identical stimuli. *Percept. Psychophys.* **71**, 5–7 (2009).
- Bernasconi, F. *et al.* Noise in Brain Activity Engenders Perception and Influences Discrimination Sensitivity. *J. Neurosci.* **31**, 17971–17981 (2011).
- Amitay, S., Irwin, A. & Moore, D. R. Discrimination learning induced by training with identical stimuli. *Nat. Neurosci.* **9**, 1446–1448 (2006).
- Cicchetti, D. V. Guidelines, criteria, and rules of thumb for evaluating normed and standardized assessment instruments in psychology. *Psychol. Assess.* **6**, 284–290 (1994).
- Gao, R., Peterson, E. J. & Voytek, B. Inferring synaptic excitation/inhibition balance from field potentials. *Neuroimage* **158**, 70–78 (2017).
- Garrett, D. D. *et al.* Moment-to-moment brain signal variability: A next frontier in human brain mapping? *Neurosci. Biobehav. Rev.* **37**, 610–624 (2013).
- Leenders, M. P., Lozano-soldevilla, D., Roberts, M. J., Jensen, O. & Weerd, P. De. Diminished Alpha Lateralization During Working Memory but Not During Attentional Cueing in Older Adults. *Cereb. Cortex* 1–12, <https://doi.org/10.1093/cercor/bhw345> (2016).
- Pfefferbaum, A., Ford, J. M., Roth, W. T. & Kopell, B. S. Age-related changes in auditory event-related potentials. *Electroencephalogr. Clin. Neurophysiol.* **49**, 266–276 (1980).
- Herrmann, B., Henry, M. J., Johnsrude, I. S. & Obleser, J. Altered temporal dynamics of neural adaptation in the aging human auditory cortex. *Neurobiol. Aging* **45**, 10–22 (2016).
- McIntosh, A. R. *et al.* Spatiotemporal dependency of age-related changes in brain signal variability. *Cereb. Cortex* **24**, 1806–1817 (2014).
- Voytek, B. & Knight, R. T. Dynamic network communication as a unifying neural basis for cognition, development, aging, and disease. *Biol. Psychiatry* **77**, 1089–1097 (2015).
- Morrison, J. H. & Hof, P. R. Life and death of neurons in the aging brain. *Science* **278**, 412–419 (1997).
- Sullivan, E. V., Rohlfing, T. & Pfefferbaum, A. Quantitative fiber tracking of lateral and interhemispheric white matter systems in normal aging: Relations to timed performance. *Neurobiol. Aging* **31**, 464–481 (2010).
- Andrews-Hanna, J. R. *et al.* Disruption of Large-Scale Brain Systems in Advanced Aging. *Neuron* **56**, 924–935 (2007).
- Geerligs, L., Rubinov, M., Cam-CAN & Henson, R. N. State and Trait Components of Functional Connectivity: Individual Differences Vary with Mental State. *J. Neurosci.* **35**, 13949–13961 (2015).
- Meunier, D., Achard, S., Morcom, A. & Bullmore, E. Age-related changes in modular organization of human brain functional networks. *Neuroimage* **44**, 715–723 (2009).
- Wang, L., Li, Y., Metzka, P., He, Y. & Woodward, T. S. Age-related changes in topological patterns of large-scale brain functional networks during memory encoding and recognition. *Neuroimage* **50**, 862–872 (2010).
- Herrmann, B., Parthasarathy, A. & Bartlett, E. L. Ageing affects dual encoding of periodicity and envelope shape in rat inferior colliculus neurons. *Eur. J. Neurosci.* **45**, 299–311 (2017).
- Caspary, D. M., Ling, L., Turner, J. G. & Hughes, L. F. Inhibitory neurotransmission, plasticity and aging in the mammalian central auditory system. *J. Exp. Biol.* **211**, 1781–1791 (2008).
- Overton, J. A. & Recanzone, G. H. Effects of aging on the response of single neurons to amplitude modulated noise in primary auditory cortex of Rhesus macaque. *J. Neurophysiol.* <https://doi.org/10.1152/jn.01098.2015> (2016).
- Curto, C., Sakata, S., Marguet, S., Itskov, V. & Harris, K. D. A simple model of cortical dynamics explains variability and state-dependence of sensory responses in urethane-anesthetized auditory cortex. *J. Neurosci.* **29**, 10600–10612 (2009).
- Boncompte, G., Villena-Gonzalez, M., Cosmelli, D. & Lopez, V. Spontaneous alpha power lateralization predicts detection performance in an un-cued signal detection task. *PLoS One* **11**, 1–13 (2016).
- Kayser, S. J., McNair, S. W. & Kayser, C. Prestimulus influences on auditory perception from sensory representations and decision processes. *Proc. Natl. Acad. Sci.* **113**, 201524087 (2016).
- Schölvinck, M. L., Saleem, A. B., Benucci, A., Harris, K. D. & Carandini, M. Cortical state determines global variability and correlations in visual cortex. *J. Neurosci.* **35**, 170–8 (2015).
- Busch, N. A., Dubois, J. & VanRullen, R. The phase of ongoing EEG oscillations predicts visual perception. *J. Neurosci.* **29**, 7869–7876 (2009).
- Strauß, A., Henry, M. J., Scharinger, M. & Obleser, J. Alpha Phase Determines Successful Lexical Decision in Noise. *J. Neurosci.* **35**, 3256–3262 (2015).

43. Wilsch, A., Henry, M. J., Herrmann, B., Maess, B. & Obleser, J. Alpha Oscillatory Dynamics Index Temporal Expectation Benefits in Working Memory. *Cereb. Cortex* **25**, 1938–1946 (2015).
44. Sams, M., Hari, R., Rif, J. & Knuutila, J. The Human Auditory Sensory Memory Trace Persists about 10 sec: Neuromagnetic Evidence. *J. Cogn. Neurosci.* **5**, 363–370 (1993).
45. Mc Evoy, L., Levänen, S. & Loveless, N. Temporal characteristics of auditory sensory memory: Neuromagnetic evidence. *Psychophysiology* **34**, 308–316 (1997).
46. Limbach, K. & Corballis, P. M. Prestimulus alpha power influences response criterion in a detection task. *Psychophysiology* **53**, 1154–1164 (2016).
47. Hesselmann, G., Kell, C. A., Eger, E. & Kleinschmidt, A. Spontaneous local variations in ongoing neural activity bias perceptual decisions. *Proc. Natl. Acad. Sci. USA* **105**, 10984–10989 (2008).
48. Amitay, S. *et al.* Human Decision Making Based on Variations in Internal Noise: An EEG Study. *PLoS One* **8**, 1–14 (2013).
49. Brainard, D. H. The Psychophysics Toolbox. *Spat. Vis.* **10**, 433–6 (1997).
50. Kothe, C. L S Layer. Available at: <https://code.google.com/archive/p/labstreaminglayer/> (2014).
51. Oostenveld, R., Fries, P., Maris, E. & Schoffelen, J.-M. FieldTrip: Open source software for advanced analysis of MEG, EEG, and invasive electrophysiological data. *Comput. Intell. Neurosci.* **2011**, 156869 (2011).
52. Shannon, C. E. A Mathematical Theory of Communication. *Bell Syst. Tech. J.* **27**, 379–423 (1948).
53. Kolmogorov, A. N. Three approaches to the quantitative definition of information \*. *Int. J. Comput. Math.* **2**, 157–168 (1968).
54. Pincus, S. M. Approximate entropy as a measure of system complexity. *Proc. Natl. Acad. Sci. USA* **88**, 2297–2301 (1991).
55. Richman, J. S. & Moorman, J. R. Physiological time-series analysis using approximate entropy and sample entropy. *Am. J. Physiol. Heart Circ. Physiol.* **278**, H2039–49 (2000).
56. Bandt, C. & Pompe, B. Permutation entropy: a natural complexity measure for time series. *Phys. Rev. Lett.* **88**, 174102 (2002).
57. Riedl, M., Müller, A. & Wessel, N. Practical considerations of permutation entropy: A tutorial review. *Eur. Phys. J. Spec. Top.* **222**, 249–262 (2013).
58. Staniek, M. & Lehnertz, K. Parameter Selection for Permutation Entropy Measurements. *Int. J. Bifurc. Chaos* **17**, 3729–3733 (2007).
59. Bédard, C., Kröger, H. & Destexhe, A. Does the 1/f frequency scaling of brain signals reflect self-organized critical states? *Phys. Rev. Lett.* **97**, 1–4 (2006).
60. Berthouze, L., James, L. M. & Farmer, S. F. Human EEG shows long-range temporal correlations of oscillation amplitude in Theta, Alpha and Beta bands across a wide age range. *Clin. Neurophysiol.* **121**, 1187–1197 (2010).
61. Maris, E. & Oostenveld, R. Nonparametric statistical testing of EEG- and MEG-data. *J. Neurosci. Methods* **164**, 177–190 (2007).
62. Wöstmann, M., Herrmann, B., Wilsch, A. & Obleser, J. Neural Alpha Dynamics in Younger and Older Listeners Reflect Acoustic Challenges and Predictive Benefits. *J. Neurosci.* **35**, 1458–1467 (2015).
63. Breakspear, M., Heitmann, S. & Daffertshofer, A. Generative Models of Cortical Oscillations: Neurobiological Implications of the Kuramoto Model. *Front. Hum. Neurosci.* **4**, 190 (2010).
64. Obleser, J., Henry, M. J. & Lakatos, P. What do we talk about when we talk about rhythm? *PLoS Biol.* **15**, e2002794 (2017).
65. Warton, D. I. & Hui, F. K. C. The arcsine is asinine: The analysis of proportions in ecology. *Ecology* **92**, 3–10 (2011).
66. Rosenthal, R. & Rubin, D. B. equivalent: A Simple Effect Size Indicator. *Psychol. Methods* **8**, 492–496 (2003).

## Acknowledgements

Research was supported by the Volkswagen foundation (to JO; BIT-CHAT) and the European Research Council (to JO; ERC-2014-CoG AUDADAPT).

## Author Contributions

L.W., M.W. and J.O. designed research. L.W. conducted experiments and analysed data with contributions from M.W. and J.O. L.W., M.W. and J.O. wrote the manuscript.

## Additional Information

**Supplementary information** accompanies this paper at <https://doi.org/10.1038/s41598-017-17766-4>.

**Competing Interests:** The authors declare that they have no competing interests.

**Publisher's note:** Springer Nature remains neutral with regard to jurisdictional claims in published maps and institutional affiliations.



**Open Access** This article is licensed under a Creative Commons Attribution 4.0 International License, which permits use, sharing, adaptation, distribution and reproduction in any medium or format, as long as you give appropriate credit to the original author(s) and the source, provide a link to the Creative Commons license, and indicate if changes were made. The images or other third party material in this article are included in the article's Creative Commons license, unless indicated otherwise in a credit line to the material. If material is not included in the article's Creative Commons license and your intended use is not permitted by statutory regulation or exceeds the permitted use, you will need to obtain permission directly from the copyright holder. To view a copy of this license, visit <http://creativecommons.org/licenses/by/4.0/>.

© The Author(s) 2017